PHYSICAL REVIEW E VOLUME 49, NUMBER 6 JUNE 1994

Topological solitons in polyethylene crystals

Fei Zhang and Michael A. Collins
Research School of Chemistry, Australian National University, Canberra, Australian Capital Territory 0200, Australia

(Received 29 November 1993)

A soliton model is presented to describe the dynamics of a single polyethylene (PE) chain surrounded by a crystal environment. The model is based on realistic intramolecular and intermolecular interactions and it generalizes the phenomenological (sine-Gordon) model proposed previously for studying the molecular mechanism underlying the dielectric relaxation of PE crystals. In the present model we obtain several types of topological soliton solutions that describe twisting and elongation (or compression) of the PE chain. It is shown that these solitons can propagate smoothly along the chain and that their interactions are inelastic.

PACS number(s): 46.10.+z, 03.40.Kf, 61.72.Bb, 63.20.Pw

I. INTRODUCTION

Over the past several years, it has become increasingly apparent that spatially localized, large amplitude nonlinear excitations contribute significantly to the physical properties of condensed-matter systems. In particular, soliton models have been widely used to describe nonlinear physical processes including DNA dynamics [1], the poling process in crystalline polyvinylidenefluoride [2], dielectric relaxation in polyethylene (PE) crystals [3–5], phase transitions in paraffin chains [6], and resonant energy transfer in molecular biology [7].

At low temperature, crystalline polyethylene chains are packed in an orthorhombic array. Each of the repeat units contains two all-*trans* planar zigzag chains. The role of various types of conformational defects created at higher temperature in these long polymer chains has been studied experimentally by examination of the bulk dielectric relaxation [8] and by spectroscopic investigations [9]. Theoretical studies of the relevant molecular dynamics at the microscopic level include calculations of conformational defects [10, 11] and molecular dynamics simulations [12–15]. In particular, some time ago Mansfield and Boyd [10] postulated the existence of *twistons*, smooth 180° twists of a PE chain accompanied with a CH_2 unit length contraction or extension of the chain extending over many CH_2 groups (far away from the twisted region the chain approaches crystallographic register asymptotically). The structure and conformation energy of the twiston have been calculated on short PE chains consisting of 22 CH_2 groups and later analyzed phenomenologically in terms of solitons [3,4]. In fact, due to the symmetry of the crystal structure, there are many equivalent ground states in the effective interchain potential. The twiston configuration connects two such ground states, thus it can be naturally described by generalized topological soliton models. However, earlier mathematical models for twistons [3, 4] have employed an oversimplified approximation for the intermolecular energy and have not explicitly taken into account the coupling between the chain twisting and translation. Recently, a more accurate intermolecular potential has been obtained and a hierarchy of twiston models has been briefly outlined [16].

In the present paper an alternative twiston (topological soliton) model is rigorously derived from realistic intra- and intermolecular interactions (Sec II). In Sec. III we obtain a π-twiston solution in the soliton model and observe good agreement with the results of direct molecular dynamics simulations. In addition, we demonstrate that a type of large amplitude excitation, namely, a 2π twist of the chain with reduced translational mismatch, collapses to a highly localized defect in the realistic system. Moreover, a kinklike solution describing pure translational dislocation of the CH_2 groups is obtained analytically and numerically. The energetics of these soliton solutions is examined in detail. Section IV is devoted to the dynamics of the solitons. It is shown that the solitons can propagate smoothly along the PE chain with very minor discreteness effects and that the interactions of two solitons are inelastic. In particular, we find that the head-on collisions of a soliton and an anti-soliton lead to annihilation unless their initial velocity exceeds a threshold value. Sec. V contains some concluding remarks.

II. MODEL

We consider the dynamics of a single PE chain constrained in the crystal environment [16]. For convenience of notation, let us first set up a right-handed reference frame XYZ, as shown in Fig. 1. The Z axis goes through the central long axis of the chain; the Y axis is perpendicular to the plane of the carbon atom chain. For the sake of simplicity each CH_2 unit is considered as a rigid group. In Fig. 1 the CH_2 units are numbered $0, 1, 2, \ldots$ from the bottom to the top. The Cartesian coordinates $\bar{X}_n = (x_n, y_n, z_n)$ and the cylindrical coordinates (r_n, ϕ_n, z_n) of the nth carbon atom have the following relation:

$$\bar{X}_n = (r_n \cos(\phi_n), r_n \sin(\phi_n), z_n). \tag{1}$$

In cylindrical coordinates, the dynamics of the reference PE chain are described by a Lagrangian:

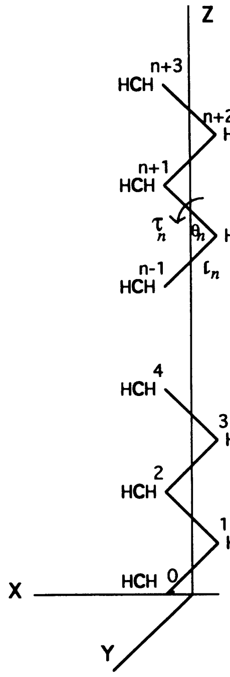

FIG. 1. Reference frame XYZ for a planar zigzag polyethylene chain. Definitions of bond length, bond angle, and torsional angle are indicated.

$$\mathcal{L} = T - U_{\text{intra}} - U_{\text{inter}}, \tag{2}$$

where T represents the kinetic energy

$$T = \frac{1}{2} m \sum_n (\dot{r}_n^2 + r_n^2 \dot{\phi}_n^2 + \dot{z}_n^2), \tag{3}$$

m being the mass of a CH_2 unit; U_{intra} is the intramolecular energy [12–15] and

$$U_{\text{inter}} = \sum_n U_e(r_n, \phi_n, z_n). \tag{4}$$

U_e is the effective potential for each CH_2 group on the central reference chain due to the whole crystal environment. It can be obtained by summing up the van der Waals interactions of a CH_2 group with all atoms on the surrounding PE chains fixed at crystal register. U_e has the following general form [16]:

$$U_e(r_n, \phi_n, z_n) = U_0(r_n, \phi_n) + U_1(r_n, \phi_n) \cos\left(\frac{\pi z_n}{c}\right), \tag{5}$$

where $c = 1.274$ Å is the spacing along the Z axis between two adjacent CH_2 units at equilibrium. Due to the symmetry of the crystal environment, $U_0(r, \phi)$ is a π-periodic function of ϕ; $U_1(r, \phi)$ is 2π periodic in ϕ. Although $U_0(r, \phi)$ and $U_1(r, \phi)$ can be approximated by Fourier series [16], the resulting forms are not simple enough to be used in an analytical treatment. However, because the variation of the coordinates r_n is rather small, even in a twisting region (see the following sections), r_n may be treated as a constant (its equilibrium value is $r_0 \approx 0.4236$ Å). Then the effective interchain potential (or substrate potential) is quite well approximated by

$$U(\phi_n, z_n) = U_0(\phi_n) + U_1(\phi_n) \cos\left(\frac{\pi z_n}{c}\right), \tag{6}$$

where

$$U_0(\phi_n) = -A_2 \cos[2(\phi_n - \phi_\epsilon)] - A_4 \cos[4(\phi_n - \phi_\epsilon)], \tag{7}$$

$$U_1(\phi_n) = B_1 \sin(\phi_n - \bar{\phi}), \tag{8}$$

with $A_2 = 0.32, A_4 = 1.48, B_1 = 1.52$ (here the energy unit is kJ/mol CH_2), $\bar{\phi} \approx 51°$, and $\phi_\epsilon = 0.038\,47 (\approx 2.204°)$ is a constant phase such that the effective potential $U(\phi, z) = U_0(\phi) + U_1(\phi) \cos(\pi z/c)$ has minima at $(\phi, z) \equiv (0, 0)$ and (π, c). The potential $U(\phi, z)$ is plotted in Fig. 2. This approximation to U_{inter} retains the essential multiminima shape which has previously been neglected in phenomenological twiston models.

Now let us turn to the intramolecular interaction U_{intra}, which is approximated by a simple sum of the energy of C-C bond stretches, C-C-C bond bends, and C-C-C-C torsions:

$$U_{\text{intra}} = \sum_n (U_{\text{bs}} + U_{\text{bb}} + U_{\text{ts}}), \tag{9}$$

where

$$E_{\text{bs}} = \frac{K_{\text{bs}}}{2} (l_n - l_0)^2, \tag{10}$$

$$E_{\text{bb}} = \frac{K_{\text{bb}}}{2} (\cos\theta_n - \cos\theta_0)^2, \tag{11}$$

$$E_{\text{ts}} = \frac{K_{\text{ts}}}{2} \sin^2 \tau_n. \tag{12}$$

The definitions of the bond length l_n, bond angle θ_n, and torsional angle τ_n are indicated in Fig. 1. These energies can be expressed in terms of the cylindical coordinates. Let (d_n, ψ_n, u_n) be the displacements of the cylindrical

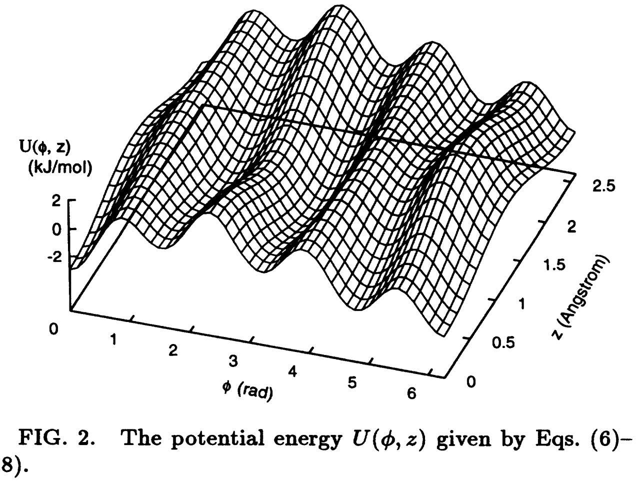

FIG. 2. The potential energy $U(\phi, z)$ given by Eqs. (6)–(8).

polar coordinates of the nth CH_2 unit from their equilibrium values, i.e.,

$$d_n = r_n - r_0, \quad \psi_n = \phi_n - \frac{1-(-1)^n}{2}\pi, \quad u_n = z_n - nc. \tag{13}$$

Suppose that $d_n, \delta\psi_n = \psi_{n+1} - \psi_n$, and $\delta u_n = u_{n+1} - u_n$ vary slowly with n, so that the continuum approximation may be used when expressing the potential energies of Eqs. (10)–(12) in terms of cylindrical coordinates. By letting $d_n = d, \delta\psi_n = \delta\psi$, and $\delta u_n = \delta u$, and keeping all second order terms we obtain

$$E_{\mathrm{bs}} \approx \frac{K_{\mathrm{bs}}}{2}\left(\frac{16r_0^2}{l_0^2}d^2 + \frac{c^2}{l_0^2}\delta u^2 + \frac{8cr_0}{l_0^2}d\,\delta u\right), \tag{14}$$

$$E_{\mathrm{bb}} \approx \frac{K_{\mathrm{bb}}}{2}\left(\frac{64r_0^2}{l_0^4}(1-\cos\theta_0)^2 d^2 + \frac{4c^2}{l_0^4}(1+\cos\theta_0)^2\delta u^2 - \frac{32cr_0}{l_0^4}\sin^2(\theta_0)\,d\,\delta u\right), \tag{15}$$

$$E_{\mathrm{ts}} \approx \frac{K_{\mathrm{ts}}}{2}\frac{1024c^2r_0^6 + 256c^4r_0^4}{l_0^8\sin^4\theta_0}\delta\psi^2. \tag{16}$$

All the parameters involved above are available from Refs. [10–15]. For convenience, they are presented here in Table I. Finally the intramolecular energy is reduced to

$$U_{\mathrm{intra}} = \frac{1}{2}\sum_n [\, K_1 d_n^2 + K_2(\psi_{n+1} - \psi_n)^2 + K_3(u_{n+1} - u_n)^2 + K_4(d_{n+1} + d_n)(u_{n+1} - u_n)], \tag{17}$$

where

$$K_1 = \frac{16r_0^2}{l_0^2}K_{\mathrm{bs}} + \frac{64r_0^2}{l_0^4}(1-\cos\theta_0)^2 K_{\mathrm{bb}} \approx 3712.655\ \mathrm{kJ/Å^2\,mol}, \tag{18}$$

$$K_2 = \frac{1024c^2r_0^6 + 256c^4r_0^4}{l_0^8\sin^4\theta_0}K_{\mathrm{ts}} \approx 109.263\ \mathrm{kJ/mol}, \tag{19}$$

$$K_3 = \frac{c^2}{l_0^2}K_{\mathrm{bs}} + \frac{4c^2}{l_0^4}(1+\cos\theta_0)^2 K_{\mathrm{bb}} \approx 1860.655\ \mathrm{kJ/Å^2\,mol}, \tag{20}$$

$$K_4 = \frac{4cr_0}{l_0^2}K_{\mathrm{bs}} - \frac{16cr_0}{l_0^4}\sin^2(\theta_0)\ K_{\mathrm{bb}} \approx 2223.384\ \mathrm{kJ/Å^2 mol}. \tag{21}$$

Combining Eqs. (2), (3), (6), and (17) we obtain a discrete Lagrangian model to describe the dynamics of a single PE chain:

$$\mathcal{L} = \frac{1}{2}m\sum_n(\dot{d}_n^2 + r_0^2\dot{\psi}_n^2 + \dot{u}_n^2) - U_{\mathrm{intra}} - U_0(\psi_n) - U_1(\psi_n)\cos\left(\frac{\pi u_n}{c}\right), \tag{22}$$

where U_{intra} is given by Eq. (17) and the functions U_0 and U_1 are given by Eqs. (7) and (8). In the following section we look for large amplitude localized excitations (solitons) in this model.

TABLE I. The intramolecular energy and model parameters.

Bond stretch energy $E_{\mathrm{bs}} = \frac{K_{\mathrm{bs}}}{2}(l - l_0)^2$ $K_{\mathrm{bs}} = 2.65 \times 10^6$ J/Å^2 mol, $l_0 = 1.53$ Å
Bond bending energy $E_{\mathrm{bb}} = \frac{K_{\mathrm{bb}}}{2}(\cos\theta - \cos\theta_0)^2$ $K_{\mathrm{bb}} = 1.3 \times 10^5$ J/mol, $\theta_0 = 112.75°$
Torsional energy $E_{\mathrm{ts}} = \frac{K_{\mathrm{ts}}}{2}\sin^2\tau$ $K_{\mathrm{ts}} = 0.7578 \times 10^5$ J/mol
Geometrical parameters $c = 1.274$ Å, $r_0 = 0.4236$ Å
Mass of a CH_2 unit $m = 14.1$ g/mol
Coefficients in the torsional potential given by Eq. (36) $a_0 = 9.279, a_1 = -12.156, a_2 = -13.120,$ $a_3 = 3.060, a_4 = 26.261, a_5 = 31.495$ (energy unit kJ/mol)

III. STATIC SOLITONS

Because the intramolecular force constants $K_i, i = 1,2,3,4$, in Eq. (17) are at least two orders of magnitude higher than those of the intermolecular potential in Eqs. (6)–(8), a continuum approximation ($n \rightarrow z/c$) can be applied to the Lagrangian model (22). Therefore, we first consider a system described by the following Lagrangian density:

$$\mathcal{L} = \frac{m}{2}(d_t^2 + r_0^2\psi_t^2 + u_t^2) - \frac{1}{2}(K_1 d^2 + K_2 c^2\psi_z^2 + K_3 c^2 u_z^2 + 2K_4 c d u_z) - U(\psi, u), \tag{23}$$

whose equations of motion are

$$m d_{tt} + K_1 d + K_4 c u_z = 0, \tag{24}$$

$$m r_0^2\psi_{tt} - K_2 c^2\psi_{zz} + \partial U/\partial\psi = 0, \tag{25}$$

$$m u_{tt} - K_3 c^2 u_{zz} - K_4 c d_z + \partial U/\partial u = 0. \tag{26}$$

Consider the static solution of Eqs. (24)–(26) by setting the derivatives of d, ψ, u with respect to time equal to zero. Then from the first equation

$$d(z) = -\frac{K_4 c}{K_1} u_z. \tag{27}$$

Substituting this equation into Eq. (26) yields

$$-K_3' c^2 u_{zz} + \partial U/\partial u = 0, \tag{28}$$

where $K_3' = K_3 - K_4^2/K_1 \approx 529.145$ kJ/mol is an effective force constant. It is easy to see that Eqs. (25) and (28) are two coupled nonlinear Klein-Gordon equations. As pointed out in Sec. II, the substrate potential $U(\psi, u)$ has many equivalent ground states. Therefore, these equations may support kinklike solutions (topological solitons) which connect two ground states of the substrate potential.

Due to the strong coupling between the two equations, it seems impossible to obtain exact analytical solutions. However, approximate solutions can be obtained due to the analogy with the well-known sine-Gordon and double sine-Gordon equations. Neglecting the coupling with u and the very small phase ϕ_ϵ, the rotation displacement ψ approximately satisfies the equation

$$-K_2 c^2 \psi_{zz} + 2A_2 \sin(2\psi) + 4A_4 \sin(4\psi) = 0, \tag{29}$$

which has an exact π-kink (antikink) solution of the form

$$\psi_\pi(z) = \pi/2 \pm \tan^{-1}\left[\eta^{-1} \sinh\left(\frac{2\eta(z - z_0)}{c\sqrt{K_2/A_2}}\right)\right], \tag{30}$$

where $\eta = \sqrt{1 + 4A_4/A_2}$ and z_0 denotes the center of the kink. Substituting Eq. (30) into Eq. (28), we may obtain an equation for the longitudinal displacement $u(z)$,

$$-K_3' c^2 u_{zz} + \frac{\pi B_1}{c} \sin[51^\circ - \psi_\pi(z)] \sin(\pi u/c) = 0, \tag{31}$$

which appears to be a sine-Gordon equation with modulated substrate potential. Since $\psi_\pi(z)$ approaches 0 and π at $z = \pm\infty$, respectively, the ground states of the substrate potential associated with Eq. (31) are $u = 0$ and $\pm c$. Therefore the solution of Eq. (31) can be approximated by

$$u(z) = \pm\frac{2c}{\pi} \tan^{-1}[\exp \gamma(z - z_0)], \tag{32}$$

where γ is a parameter characterizing the width of the kink, which can be estimated by a variational method [17]. Here for the sake of simplicity, γ is approximated by $\frac{\pi}{c^2}\sqrt{B_1/K_3'}$. From Eqs. (27) and (32) we obtain the displacement

$$d(z) = \pm\frac{K_4 \gamma c^2}{K_1 \pi} \frac{1}{\cosh[\gamma(z - z_0)]}. \tag{33}$$

Thus $d(z)$ has a bell shape which decays exponentially away from the soliton center. Note that $\gamma \ll 1$ and $K_4 \sim K_1$, so the displacement given by Eq. (33) is rather small indeed. This is consistent with our assumption in Sec. II that the variation of the coordinates r_n is negligible.

The analytical solution given by Eqs. (30), (32), and (33) is presented in Fig. 3 and compared with a numerical solution of the discrete model, Eq. (22), obtained using a molecular dynamics simulation with damping. The agreement between analytical and numerical results is fairly good.

Equations (30), (32), and (33) describe a *localized twist* (twiston) of the PE chain. In particular, $\psi_\pi(z)$, which goes from zero to π and occupies about 14 CH_2 units, describes the rotation of the PE chain around its long central axis; $u(z)$ represents the translational mismatch accompanied with the twist (hereafter this type of solution is named a π twiston). It is easy to check that the solution $[\psi_\pi(z), u(z)]$ indeed connects two ground states, $(0, 0)$, and $(\pi, \pm c)$ of the potential $U(\psi, u)$. In other words, the chain goes back to crystal register asymptotically far away from the twisted region.

Furthermore, the energy of the twiston described by Eqs. (30), (32), and (33) is calculated to be 82.53kJ/mol, while the numerical solution of the discrete model gives an energy of 81.21 kJ/mol. These two values are in excellent agreement with each other, showing again the validity of the analytical solution based on the continuum approximation.

Another type of large amplitude excitation in the sys-

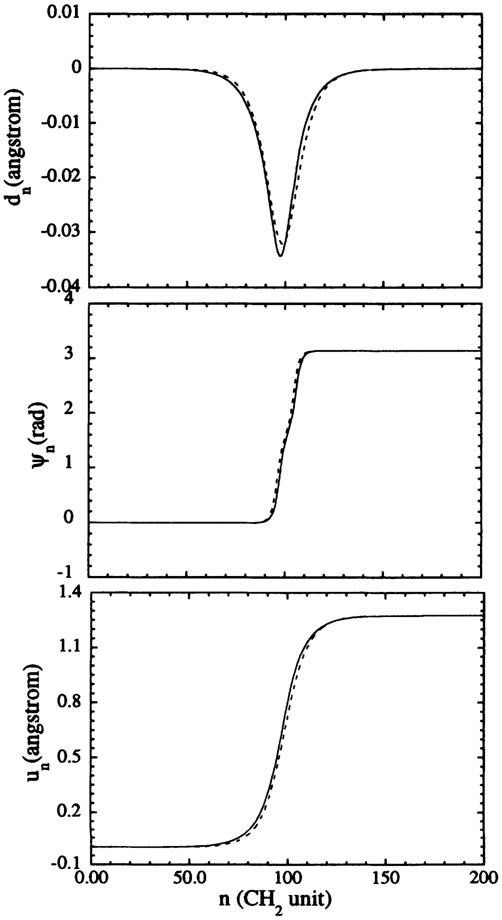

FIG. 3. The twiston solution given by Eqs. (30), (32), and (33) based on the continuum approximation (dashed line), which is in good agreement with the numerical solution of the discrete model, Eq. (22) (solid line).

tem (24)–(26) is a 2π twist with virtually no translational mismatch. Setting $u = 0$ and $d = 0$ in Eq. (25) yields

$$-K_2c^2\psi_{zz} + 2A_2\sin[2(\psi - \phi_\epsilon)] + 4A_4\sin[4(\psi - \phi_\epsilon)] + B_1\cos(\psi - 51^\circ) = 0. \quad (34)$$

The ground states of the substrate potential associated with Eq. (34) are $2k\pi$, $k = 0, \pm 1, \pm 2, \ldots$. Thus Eq. (34) admits 2π-kink solutions, which describe a 360° twist of the PE chain. The energy of the 2π twiston is found to be about 152.02 kJ/mol, less than *double* the energy of the π twiston.

In addition to these twistons, another static soliton-like solution of Eqs. (24)–(26) can be obtained by setting $\psi \approx 0$. In this case, $u(z)$ approximately satisfies a sine-Gordon equation

$$-K_3'c^2u_{zz} + \frac{\pi B_1\sin(51^\circ)}{c}\sin\left(\frac{\pi u}{c}\right) = 0, \quad (35)$$

whose kinklike solutions are wellknown. However since $K_3' \gg \pi B_1\sin(51^\circ)/c$, the width of this kink will be very large. Numerical calculations show that the $2c$ kinks, which are related to a $2c$ elongation or compression of the chain, spread over about 30 CH_2 units and that their energy is about 80.36 kJ/mol. This is slightly less than the energy of the π twiston.

In order to check the above results that are obtained from the soliton model, we have performed molecular dynamics calculations for a complete model using the more accurate interchain interactions [16], the bonded interactions of Eqs. (10) and (11), and the realistic torsional potential [12–15]

$$E_{\text{tors}}(\tau) = \sum_{i=0}^{5} a_i\cos^i(\tau). \quad (36)$$

The coefficients a_i are presented in Table I, and this torsional potential is shown in Fig. 4. Note that a simple quadratic approximation of Eq. (36) about the minimum yields Eq. (12).

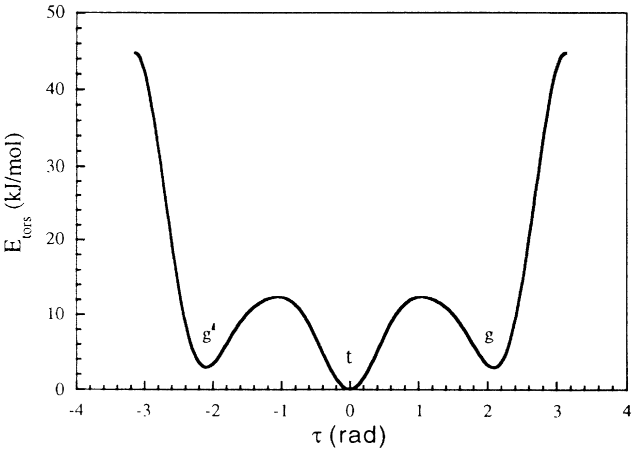

FIG. 4. The more realistic torsional potential given by Eq. (36).

Using molecular dynamics simulation with damping, it has been found that the π twiston in the complete model has an energy around 72 kJ/mol, which is in good agreement with that found in the soliton model. Moreover, the configuration of the π twiston obtained in the more realistic model is found to be virtually the same as in the soliton model of Eq. (22). Similar agreement is observed for the $2c$ kinks that describe the $2c$ elongation or compression of the PE chain.

However, when using a 2π twiston configuration as an initial condition in the molecular dynamics simulations, we find that it converges to an extremely localized twist containing two *gauche* conformations as indicated in Fig. 5. The realistic torsional energy, Eq. (36), has local minima at the *gauche* conformations $g(\tau = 120^\circ)$, and $g'(\tau = -120^\circ)$. The energy difference between the *gauche* and *trans* ($\tau = 0$) conformations is rather small, only about 2.825 kJ/mol (see Fig. 4). The *gttg* defect in Fig. 5 (see the lower graph) has an energy of about 78.46 kJ/mol, much less than that of the 2π twiston in the soliton model. Here we would like to point out that *gauche* defects are the most populous ones in high temperature PE crystals due to their low conformational

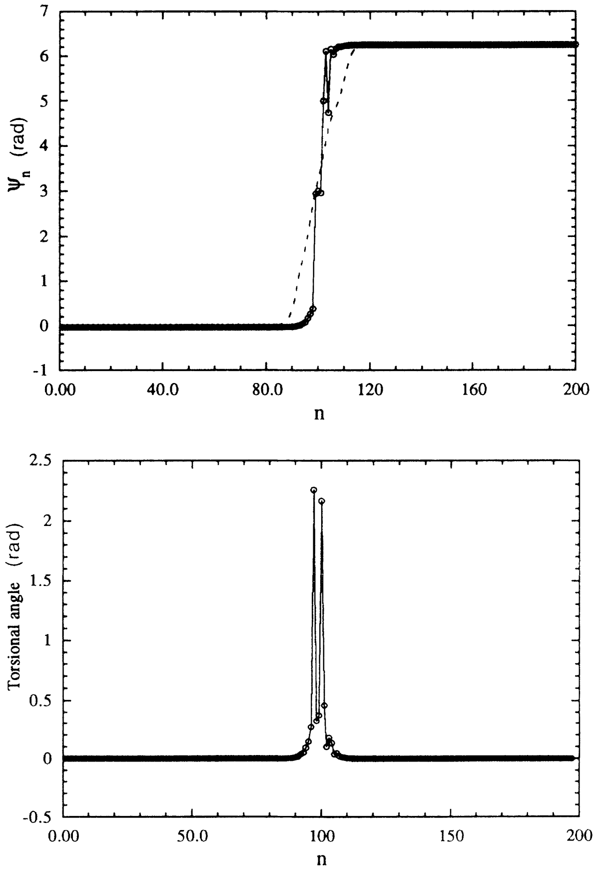

FIG. 5. The 2π-kink solution of Eq. (34) (dashed line). The solid lines with circles are the numerical simulation results based on the complete model (see text). Note that the torsional angle (shown in the lower graph) contains two *gauche* conformations, which represent two sharp twists of the PE chain.

energy [12–15]. Unlike the smooth π twistons, these *gauche*-containing defects cannot move smoothly on the PE chain.

IV. DYNAMICS OF THE SOLITONS

Once we have obtained the conformation of the solitons on a single PE chain, it is interesting to investigate their dynamics. First note that the speeds of small amplitude linear waves in Eqs. (25) and (26) are $C_1 = \sqrt{K_2c^2/(mr_0^2)} \approx 8.37 \times 10^3$ m/s and $C_2 = \sqrt{K_3c^2/m} \approx 1.32 \times 10^4$ m/s. So, the speed limit of the solitons is $C_1 \sim 10^4$ m/s.

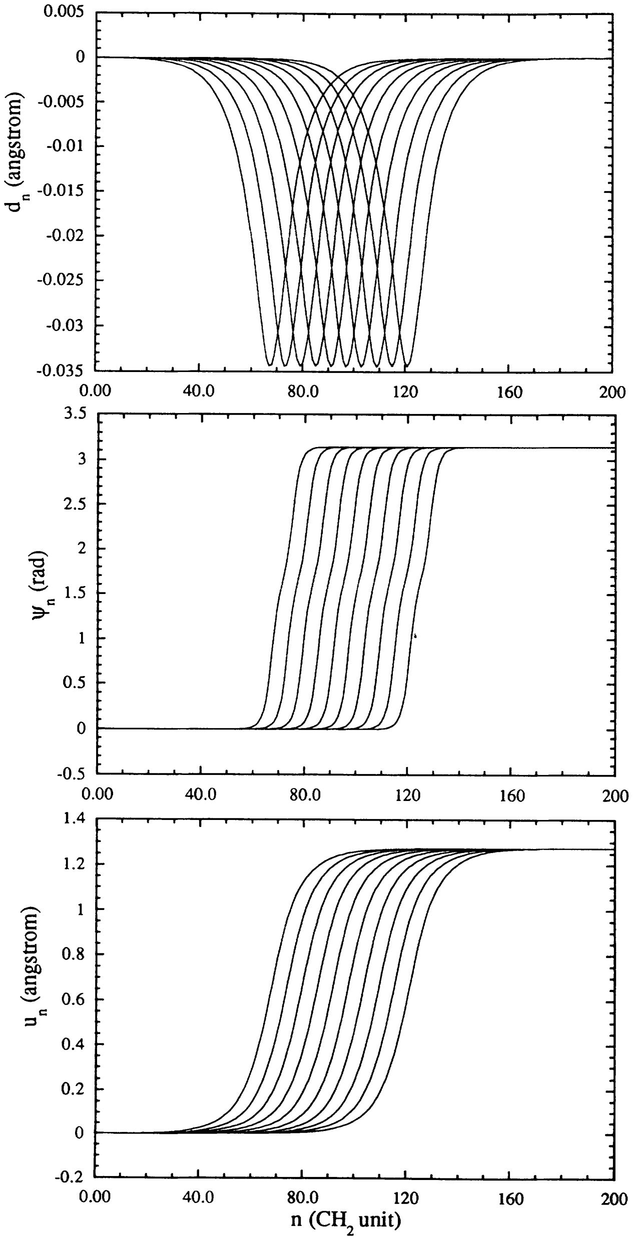

FIG. 6. Propagation of a π twiston at velocity $v = 3c$/ps ($c = 1.274$ Å) is represented by the CH_2 group coordinates at successive times.

Discreteness effects (such as the Peierls-Nabarro potential barrier) are common features in nonintegrable discrete soliton-bearing systems [18]. However such effects in the present soliton model, Eq. (22), are negligible since the intramolecular interactions are far stronger than the interchain forces. Therefore the solitons should be able to propagate through the chain rather smoothly, with no local hopping barrier. To verify this, we have carried out simulations of the solitons at different velocities ranging from 1 Å/ps to 60 Å/ps. It was found that the solitons can indeed propagate freely with constant (nonzero) velocity. Figure 6 shows a numerical simulation of the propagation of a π twiston with velocity $v = 3c$/ps ($\approx$ 3.82 Å/ps).

Now consider the interaction of two π twistons. Topologically, there are *four* types of initial configurations for the collisions as shown in Fig. 7. It was found numerically

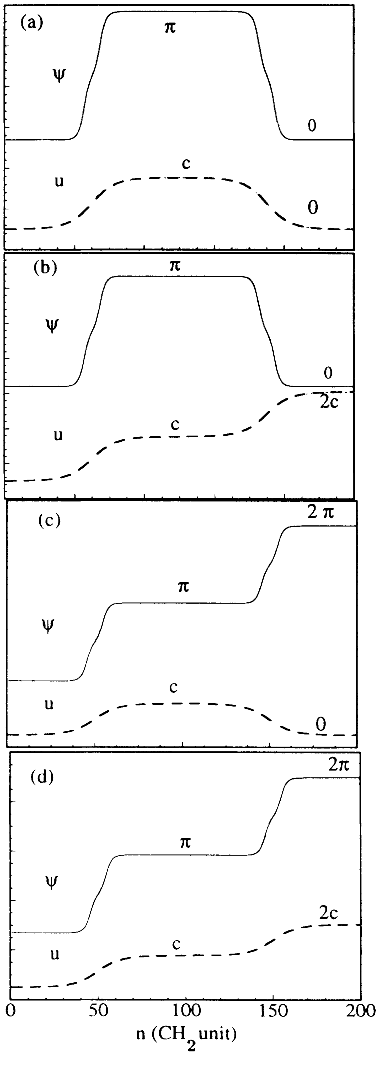

FIG. 7. Four types of initial configurations for the head-on collisions of π twistons. Only ψ_n and u_n are illustrated schematically: (a) twist elongation–antitwist compression; (b) twist elongationan–antitwist elongation; (c) twist elongation–twist compression; (d) twist elongation–twist elongation.

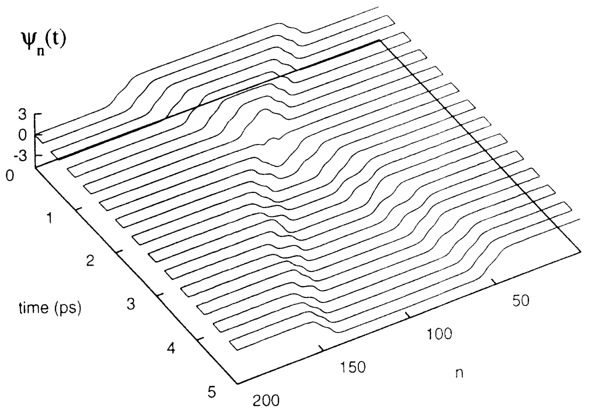

FIG. 8. Head-on collision of a π twiston and an anti-π twiston at initial velocity $v = 35c$/ps. They pass through each other (only ψ_n is shown here).

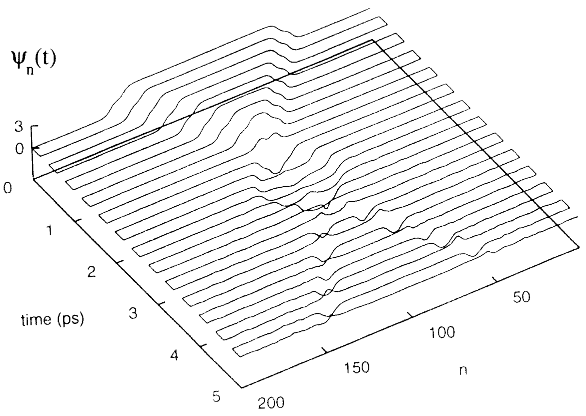

FIG. 9. Head-on collision of a π twiston and an anti-π twiston at initial velocity $v = 33c$/ps. Annihilation of the twistons is observed.

that all the collisions are strongly inelastic, generating a lot of small amplitude waves. Note that the inelasticity of such collisions is a common feature of some *nonintegrable* soliton systems [19].

Some possible results of these collisions may be anticipated qualitatively from a purely topological point of view. Here we summarize the numerical simulation results for equal-velocity *head-on* collisions.

(i) For the first type of interaction [Fig. 7(a)], there exists a threshold volocity $v_1 \approx 34c$/ps, such that if the incoming velocity of the twistons is larger than this threshold value, the twistons will pass through each other (Fig. 8) with reduced final velocity (as part of their kinetic energy is lost through radiation). On the contrary, if their incoming velocity is lower than the threshold, the collision will result in mutual annihilation (Fig. 9).

(ii) For the second type of initial condition [Fig. 7(b)], the twistons can emerge from the collision if their initial velocity is higher than a threshold value $v_2 \approx 40c$/ps, while at lower initial velocities they form a $2c$ kink, which is related to a pure elongation or compression of the PE chain.

(iii) For the third type of interaction [Fig. 7(c)], the two colliding twistons may pass through each other if their initial velocity is larger than a threshold $v_3 \approx 15c$/ps. However, a 2π twiston is formed at lower velocity collisions.

(iv) As to the fourth type of collision, the two twistons are strongly repulsive to each other and mutual annihilation is impossible topologically. The twistons always reflect each other inelastically.

We have also examined the interactions of two $2c$ kinks (that correspond to chain compression or elongation). Since these solitons are described approximately by a sine-Gordon equation [cf. Eq. (35)], their interactions are expected to be more elastic than the twiston interactions. In particular, it is found that a $2c$ kink and an anti-$2c$ kink may pass through each other easily. The critical initial velocity for passing is found to be about $v_p = 5c$/ps.

Because 2π twistons collapse to highly localized (immobile) defects in realistic PE chains, we have not studied their dynamics in the context of a soliton model.

V. CONCLUDING REMARKS

Topological solitons may represent a general class of large amplitude excitations in crystalline polymers. Due to the periodicity of the crystal structure, the interchain interactions can be effectively approximated by periodic functions [16], while the strong intramolecular interactions (bond stretch, bond bend, etc.) can be expanded in terms of suitable displacements of the atoms. Therefore, a continuum model of the chain motion would naturally be related to generalized nonlinear Klein-Gordon equations. In the simplest cases, the well-known sine-Gordon or double sine-Gordon equation may be employed as a phenomenological model to describe the twisting dynamics of flexible polymer chains (see, e.g., [2, 4, 6, 16]).

Here we have presented a twiston (soliton) model for a single PE chain surrounded by the crystal environment. Based on this model, three types of topological solitons have been found analytically and numerically. In particular, the π twistons describe a 180° twist of the chain with one CH_2 unit length mismatch, similar to that originally proposed by Mansfield and Boyd [10]. A 2π twiston is stable in the simple soliton model, but collapses to a highly localized *gttg* defect when the torsion potential takes the realistic form [12]. In addition, a stable soliton exists for pure elongation or compression of the chain. Surprisingly, perhaps, the energy of this object is comparable to that of the better known π twiston. In comparison with the original calculation of Mansfield and Boyd [10], the present soliton model yields a significantly higher energy for the π twistons. This appears to be almost solely due to the use here of a larger force constant for the torsion K_2. We note that our value of K_2 is consistent with the more realistic torsion potential [12, 13]. Using the smaller value of K_2 [3, 10] in our model yields an energy for the π twiston close to that found earlier.

The propagation of a π twiston from one chain end to the other results in a CH_2 unit length translation; thus the creation and motion of π twistons have been suggested as a justification for the surface roughening in the α phase of PE crystals [9]. Surface roughening may also be produced by propagation of the $2c$ kinks. Not only are these kinks of comparable energy to the π twiston, but by collision, two π twistons can annihilate (the twist) to produce these $2c$ kinks. Therefore, the existence of $2c$ kinks may provide an alternative explanation for the surface roughening observed experimentally and numerically in the α phase of PE crystals.

[1] S.M. Englander *et al.*, Proc. Natl. Acad. Sci. U.S.A. **77**, 7222 (1980); S. Homma and S. Takeno, Prog. Theor. Phys. **72**, 679 (1984); M. Peyrard and A.R. Bishop, Phys. Rev. Lett. **62**, 2755 (1989); L.V. Yakushevich, Phys. Lett. A **136**, 413 (1989); V. Muto, P.S. Lomdahl, and P.L. Christiansen, Phys. Rev. A **42**, 7452 (1990); V. Muto, A.C. Scott, and P.L. Christiansen, Physica D **44**, 75 (1990); G.F. Zhou and C.T. Zhang, Phys. Scr. **43**, 347 (1991).

[2] H. Dvey-Aharon, T.J. Sluckin, P.L. Taylor, and A.J. Hopfinger, Phys. Rev. B **21**, 3770 (1980).

[3] M.L. Mansfield, Chem. Phys. Lett. **69**, 383 (1980).

[4] J.L. Skinner and P.G. Wolynes, J. Chem. Phys. **73**, 4015 (1980); J.L. Skinner and Y.H. Park, Macromolecules **17**, 1735 (1984).

[5] K. J. Wahlstrand, J. Chem, Phys. **82**, 5247 (1985); K.J. Wahlstrand and P.G. Wolynes *ibid.*, **82**, 5259 (1985).

[6] K. Fukao, J. Chem. Phys. **92**, 6867 (1990); P. Sozzani, F.A. Bovey, and F.C. Schilling, Macromolecules **24**, 6764 (1991).

[7] D.J. Clarke and M.A. Collins, J. Chem. Phys. **92**, 5602 (1990); **93**, 7894 (1990); Biophys. J. **61**, 316 (1992).

[8] R.H. Boyd, Polymer **26**, 323 (1985); **26**, 1123 (1985).

[9] G. Zerbi and M.D. Zoppo J. Chem. Soc. Faraday Trans. **88**,1835 (1992); M.D. Zoppo and G. Zerbi, Polymer **33**, 4667 (1992).

[10] M.L. Mansfield and R.H. Boyd, J. Polym. Sci. Phys. Ed. **16**, 1227 (1978).

[11] D.H. Reneker and J. Mazur, Polymer **24**,1387 (1983); **29**, 3 (1988).

[12] J.P. Ryckaert and M.L. Klein, J. Chem. Phys. **85**, 1613 (1986); J.P. Rychaert, I.R. McDonald, and M.L. Klein, Mol. Phys. **58**, 698 (1989).

[13] T. Yamamoto and Y. Kimikawa, J. Chem. Phys. **97**, 5163 (1992); **99**, 6126 (1993).

[14] B.G. Sumpter, D. W. Noid, and B. Wunderlich, J. Chem. Phys. **93**, 6875 (1990); Macromolecules **23**, 4671 (1990); **25**, 7247 (1992).

[15] D.W. Noid, B.G. Sumpter, and B. Wunderlich, Macromolecules **23**, 664 (1990); **24**, 4148 (1991).

[16] F. Zhang and M.A. Collins, Chem Phys. Lett. **214**, 459 (1993).

[17] O.M. Braun, F. Zhang, Yu.S. Kivshar, and L. Vazquez, Phys. Lett. A **157**, 241 (1991).

[18] M. Peyrard and M.D. Kruskal, Physica D **14**, 88 (1984); R. Boesch and C.R. Willis, Phys. Rev. B **39**, 361 (1989); Yu.S. Kivshar and D.K. Campbell, Phys. Rev. E **48**, 3077 (1993).

[19] M.J. Ablowitz, M.D. Kruskal, and J.F. Ladik, SIAM J. Appl. Math. **36**, 428 (1979); D.K. Campbell, J.F. Schofeld, and C.A. Wingate, Physica D **9**, 1 (1983); M. Peyrard and D.K. Campbell, *ibid.* **9**, 33 (1983); D.K. Campbell, M. Peyrard, and P. Sodano, *ibid.* **19**, 165 (1986).